Laser and Particle Beams (2002), *20*, 223–226. Printed in the USA.

DOI: 10.1017/S0263034602202104

Analysis of space-resolved X-ray spectra from laser plasmas

L. LABATE,[1,2] M. GALIMBERTI,[1,3] A. GIULIETTI,[1] D. GIULIETTI,[1,3]
L.A. GIZZI,[1] AND R. NUMICO[1]

[1]Intense Laser Irradiation Laboratory, IPCF (CNR), Pisa, Italy
[2]Dipartimento di Fisica, Università di Bologna, Bologna, Italy
[3]Dipartimento di Fisica, Università di Pisa and INFM, Unità di Pisa, Italy

(RECEIVED 15 November 2001; ACCEPTED 9 December 2001)

Abstract

High dynamic range, space-resolved X-ray spectra, obtained using a TlAP crystal and a cooled CCD camera as a detector, were used to investigate the electron density and temperature profiles of an aluminum laser plasma with micrometer resolution. The electron density profile retrieved from the measurements is compared with numerical predictions from the two hydrodynamics codes MEDUSA (1D) and POLLUX (2D). It is shown that 2D density profiles can be successfully reproduced by 1D simulations using a spherical geometry with an ad hoc initial radius, leading to similar electron temperature profiles.

Keywords: Laser plasma X-ray emission; Plasma hydrodynamics; X-ray spectroscopy

1. INTRODUCTION

Plasmas produced by focusing laser pulses on solid targets are of great interest for both basic physics studies and applications. It is then essential that such plasmas can be accurately described in their fundamental parameters, namely electron density and temperature. Very accurate characterization can be achieved with combined measurements obtained by optical probing interferometry and X-ray spectra (Giulietti & Gizzi, 1998). This has been done successfully, for example, in the case of underdense plasmas produced with the laser exploding foil technique (Gizzi *et al.*, 1994; Borghesi *et al.*, 1996). In that case, the electron density map at a given time and the temperature evolution were found. However, in the case of plasmas produced by solid targets, optical probing is limited to the outer region of the plasma, far from the critical region. In this case, additional information must be gained by other diagnostics or by space-resolved X-ray spectroscopy. A first trial in this direction was done by simply comparing X-ray and second harmonic emission (Giulietti *et al.*, 1998). Here we present the progress on the characterization method of plasmas produced with nanosecond laser pulses, based on space-resolved X-ray spectroscopy. The laser pulse duration allows the plasma to be considered basically stationary for most of the pulse duration, during which most of the X-ray emission takes place. For this reason, we can use time-integrated X-ray spectra without significant loss of information. The experimental technique for detection of spatially resolved X-ray spectra from laser plasma has been described in a previous paper (Labate *et al.*, 2001), and will be briefly recalled below. This paper focuses on the discussion of the use of numerical codes for plasma characterization starting from space-resolved X-ray spectra.

Address correspondence and reprint requests to: Luca Labate, Intense Laser Irradiation Laboratory, CNR, Pisa, Italy. E-mail: luca@ifam.pi.cnr.it

2. EXPERIMENTAL SETUP

The plasma was generated by irradiating a thick Al target using a 3 ns FWHM Nd:YLF laser ($\lambda = 1.053\ \mu$m), focused by means of an $f/4$ optics. An equivalent plane setup was employed in order to monitor the spatial extent of the beam for different focusing conditions on the target. The focal spot size was measured to be approximately 10 μm; we used this value in the 2D simulations performed by the hydrodynamics code POLLUX, as explained below. Since the energy of the laser pulse is about 3 J per shot, this gives an intensity on target of about 5×10^{14} W/cm^2. The spectrometer consisted of a thallium hydrogen phthalate (TlAP) flat

crystal ($2d = 25.9$ Å), used in a first-order Bragg configuration, as a dispersive element and a back-illuminated Peltier-cooled CCD camera as a detector. Due to the high S/N ratio (dynamic range) of the CCD, we were able to acquire clear spatially resolved spectra by inserting a narrow (10 μm) slit between the plasma and the crystal. Due to the geometrical constraints, the spatially resolved axis could not be made to coincide with one of the main axes of the interaction geometry. We therefore used geometrical consideration during the data analysis to retrieve the plasma electron density and temperature profiles along the longitudinal direction, that is, along the normal to the target, corresponding to the plasma main expansion direction. The overall spatial resolution was estimated to be about 20 μm.

The spectrometer was mounted so as to obtain spectra in the range from 5.5 to 8 Å. This spectral range covers the main resonance lines from lithium-, helium-, and hydrogen-like aluminum ions. The obtained spectral resolution, essentially limited by the source size, was $\delta\lambda/\lambda \approx 2 \times 10^{-3}$.

3. DENSITY AND TEMPERATURE PROFILE RETRIEVAL

Figure 1 shows schematically the main steps of the retrieval method. The space-resolved X-ray spectrum of the plasma has been used to retrieve the plasma electron density and temperature by comparison of the experimental line ratios with the predictions of the atomic physics code RATION (Lee *et al.*, 1984). This code solves the rate equations for the lower levels of the ionization stages of the plasma in collisional-radiative equilibrium, necessary to calculate spectral line ratios as a function of plasma density and temperature, taking into account the re-absorption effects for an optically thick plasma. This requires the knowledge of the plasma size along the line of sight. This point has already been discussed previously (Labate *et al.*, 2001). Here we compare experimental data and hydrodynamics simulations performed using two different codes.

To obtain both the electron density and temperature from spectroscopic measurements at least two independent line ratios are needed. We used Lyα-to-Heβ and Heα-to-IC intensity ratios. The intercombination line (IC) results from the $1s2p\ ^3P \rightarrow 1s^2\ ^1S$ transition in the Al XII ions. Figure 5 of Labate *et al.* (2001) shows the spatial behavior of these two line ratios along the normal to the target (z-axis), up to about 350 μm from the target original surface. Together with the estimate for the plasma thickness along the line of sight, the two line ratios allowed us to attribute a nearly constant electron temperature of about 650 eV for the region $z \gtrsim 200$ μm from the target surface. A similar estimate, leading to an electron temperature of about 200 eV, was also possible for the region $z \lesssim 75$ μm. In the intermediate region, however, we failed in estimating the temperature, due to its dramatic dependence upon the plasma size. Analogously, the electron density profile was estimated, which gave a density value greater than the critical density ($n_{c@1\mu m} \approx 10^{21}$ cm^{-3}) for the region $z \lesssim 75$ μm and a value of the order of 10^{20} cm^{-3} for $z \gtrsim 200$ μm.

4. DENSITY PROFILE: EXPERIMENTAL DATA VERSUS HYDRODYNAMIC SIMULATIONS

We first compare the density values obtained from the line ratios with hydrodynamic simulations performed with the 1D Lagrangian code MEDUSA (Christiansen *et al.*, 1974; Rodgers *et al.*, 1989), attempting to complete the evaluation of the density profile over the whole plasma region we have investigated. The electron density profile of the plasma predicted by the 1D code (in *plane geometry*) at the peak of the laser pulse is shown in Figure 2 (solid line). The profile is nearly flat over the entire region, in contrast with the experimental data. If we assume this density profile for temperature calculation with RATION, we obtain a constant temperature of about 200 eV. A different result is obtained with the same code running in spherical geometry. The radius of the virtual spherical target, $r = 100$ μm, was chosen in order to match the experimental values of the density in the two extreme regions (the closest and the farthest from the target we could get). As shown in Labate *et al.* (2001), changing the target radius results in a change of the density

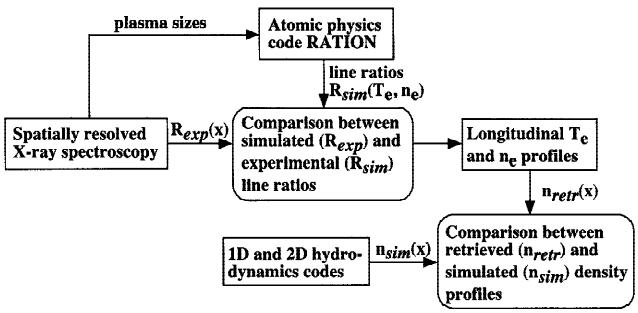

Fig. 1. Diagram of the main steps of the electron density and temperature retrieval method.

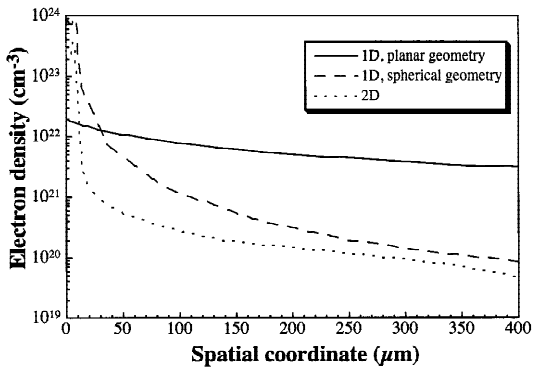

Fig. 2. Electron density at the peak of the laser pulse obtained by hydrodynamic 1D (with planar and spherical geometry) and 2D simulations.

profile in the region near to the target. The result is plotted in Figure 2 (dashed line).

To check the validity of this "modified" profile, we performed a 2D simulation of the hydrodynamic expansion of the plasma, using the eulerian code POLLUX (Pert, 1981). The same input parameters were used as for the MEDUSA code. The laser intensity was assumed to be Gaussian with a FWHM of 10 μm. The longitudinal electron density profile is shown in Figure 2 (dotted line). Of course some differences still exist between the simulation obtained with the 1D code using the spherical geometry and with the 2D code. The discrepancy between the two simulations is greater in the region closer to the original target surface, where the actual expansion of the plasma cannot be described by a 1D, although spherical, simulation. The two simulations then give similar density values at distances from the target greater than about 200 μm. Nevertheless, the two profiles lead to similar results for the electron temperature, as shown below.

5. TEMPERATURE PROFILE

The knowledge of the spatial behavior of the Lyα-to-Heβ intensity ratio as obtained from X-ray spectra allows us to retrieve a longitudinal profile of the electron temperature of the plasma, provided that an independent line intensity ratio, such as the Heα-to-IC, is used to obtain the density profile. Unfortunately, as discussed above, we were not able to get detailed temperature and density profiles by only pure spectroscopic measurements, but only an estimate of the values of temperature and density in the extreme regions of the examined spatial interval. Therefore the density profiles as given by the hydrodynamic simulations, obtained as explained in the preceding section, were used for the evaluation of the entire temperature profile. Figure 3 shows the temperature profiles of the plasma retrieved assuming the density profile obtained by the 1D code in the spherical geometry and that obtained by the 2D code. Clearly, although the behavior of the electron temperature is different in the intermediate region, nearly the same values were obtained for the temperature in the overdense region near the target (about 200 eV) and for the coronal region (about 650 eV). These values of the electron temperature are much smaller than those obtained, at the peak of the laser pulse, from the hydrodynamic simulations performed with MEDUSA, both using planar and spherical geometry, although the latter gives much lower values. Much more reasonable values were obtained by POLLUX, which predicted for the region between 200 and 400 μm a nearly constant temperature of about 800 eV, which is about 20% higher than that retrieved from the experimental data. In general, we can say that a good agreement was obtained for the electron density between the hydrodynamic simulations and the experimental data, while the agreement was much worse with the simulated temperature profile. A similar behavior was also observed by Young *et al.* (1988) using experimental data from free-bound recombination continuum in Al XIII ions.

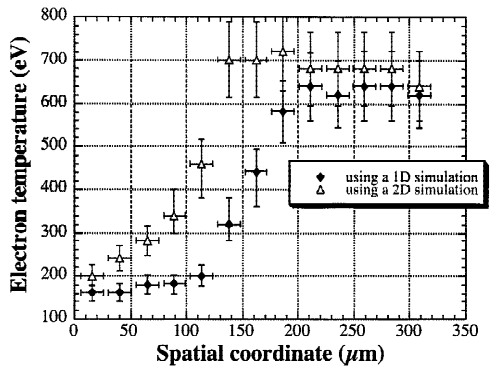

Fig. 3. Electron temperature profiles obtained by spectroscopic measurements assuming density profiles simulated by a 1D code with spherical geometry and by a 2D code.

6. SUMMARY AND CONCLUSIONS

We reported on the analysis we have performed on spatially resolved spectra of an aluminum laser plasma, obtained using a flat crystal spectrometer coupled to a narrow slit and a back-illuminated cooled CCD as a detector. Experimental data, together with the predictions of an atomic physics code, reveal an electron density profile much steeper than that indicated by planar 1D hydrodynamic simulations. This observation led us to modelling our experimental data, in order to take into account the transverse expansion of the plasma, with the same 1D code but using a spherical geometry instead of a planar one. We then compared this modified profile with that obtained using a 2D hydrodynamics code, finding a satisfactory agreement. Further, the electron temperature profiles which can be retrieved from the spectroscopic measurements in the two cases both give the same electron temperature for the coronal region (about 650 eV) and for the colder region near to the target (about 200 eV). Further improvements of this technique, eventually using spherical crystals (Blasco *et al.*, 2001), can also enable similar studies on shorter pulse plasmas.

ACKNOWLEDGMENTS

We would like to thank A. Barbini, A. Rossi, A. Salvetti, and W. Baldeschi for their invaluable technical assistance. We also acknowledge financial support from the European Research Training Network XPOSE Contract No. HPRN-CT-2000-00160.

REFERENCES

Blasco, F., Stenz, C., Salin, F., Faenov, A.Ya., Magunov, A.I., Pikuz, T.A. & Skobelev, I.Yu. (2001). Portable, tunable, high-luminosity spherical crystal spectrometer with X-ray

Charge Coupled Device for high-resolution X-ray spectromicroscopy of clusters heated by femtosecond laser pulses. *Rev. Sci. Instr.* **72**, 1956–1962.

Borghesi, M., Giulietti, A., Giulietti, D., Gizzi, L.A., Macchi, A. & Willi, O. (1996). Characterization of laser plasmas for interaction studies: Progress in time-resolved density mapping. *Phys. Rev. E* **54**, 6769–6773.

Christiansen, J.P., Ashby, D.E. & Roberts, K.V. (1974). MEDUSA—A one-dimensional laser fusion code. *Comput. Phys. Commun.* **7**, 271–287.

Giulietti, A., Beneduce, C., Ceccotti, T., Giulietti, D., Gizzi, L.A. & Mildren, R. (1998). Study of second harmonic emission for characterization of laser-plasma X-ray sources. *Laser Part. Beams* **16**, 397–404.

Giulietti, D. & Gizzi, L.A. (1998). X-ray emission from laser-produced plasmas. *Riv. Nuovo Cimento* **21**, 1–93.

Gizzi, L.A., Giulietti, D., Giulietti, A., Afshar-rad, T., Biancalana, V., Chessa, P., Danson, C., Schifano, E., Viana, S.M. & Willi, O. (1994). Characterization of laser plasmas for interaction studies. *Phys. Rev. E* **49**, 5628–5643.

Labate, L., Galimberti, M., Giulietti, A., Giulietti, D., Gizzi, L.A., Numico, R. & Salvetti, A. (2001). Line spectroscopy with spatial resolution of laser-plasma X-ray emission. *Laser Part. Beams* **19**, 117–123.

Lee, R.W., Whitten, B.L. & Stout, R.E. (1984). SPECTRA—A model for K-shell spectroscopy. *J. Quant. Spectrosc. Radiat. Transfer* **32**, 91–101.

Pert, J. (1981). Algorithms for the self-consistent generation of magnetic fields in plasmas. *J. Comput. Phys.* **43**, 111–163.

Rodgers, P.A., Rogoyski, A.M. & Rose, S.J. (1989). MED101: A laser-plasma simulation code. User guide. RAL Report No. RAL-89-127. Rutherford Appleton Laboratory.

Young, B.K.F., Stewart, R.E., Cerjan, C.J., Charatis, G. & Busch Gar, E. (1988). Time-resolved measurement of coronal temperature and line-intensity profiles in laser-produced plasmas. *Phys. Rev. Lett.* **61**, 2851–2854.